Reversible Digitally Filtered Molecular Dynamics

Stephen C. Phillips, Martin T. Swain, Adrian P. Wiley, and Jonathan W. Essex*

Department of Chemistry, University of Southampton, Highfield, Southampton, SO17 1BJ, UK

Colin M. Edge

GlaxoSmithKline, New Frontiers Science Park (North), Coldharbour Road, Harlow, CM19 5AD, UK

Received: July 8, 2002; In Final Form: December 6, 2002

It has recently been shown that digital filtering methods may be used to selectively enhance or suppress the vibrational motion in a molecular dynamics computer simulation solely on the basis of frequency (*J. Chem. Phys.* **2000**, *112*, 2586−2597). The method of digitally filtered molecular dynamics (DFMD) does, however, suffer from a number of disadvantages, the most important of which is the rapid redistribution of energy from the selected frequency range in condensed phase simulations. Here, an extension of the DFMD method that solves this problem, reversible digitally filtered molecular dynamics (RDFMD), is presented. In RDFMD, the digital filter is applied successively to velocities that have been generated from previous applications of the filter, by the simple expedient of running simulations both forward and backward in time to fill the filter buffer after each filter application. In this way, kinetic energy is added slowly to the system, with the result that the conformational transitions observed are more controlled and realistic. The method is applied to a number of systems of increasing complexity including alanine dipeptide in gas and condensed phases. These studies demonstrate the advantage of adding energy gradually and also reveal a change in the characteristic frequency of critical vibrations as the transition state is approached. A protocol for applying RDFMD to protein systems has also been devised and tested on the YPGDV pentapeptide in water.

1. Introduction

The length of molecular dynamics (MD) simulations has increased to a point where multiple-nanosecond simulations of large, solvated protein systems are routine. However, to adequately study conformational change in a protein and therefore fully understand its function, a simulation time-scale of the order of milliseconds to seconds may be necessary.[1] Techniques to increase the conformational space sampled during the limited time-scale of current MD simulations may be split into those that drive the MD from one structure to another (including the self-penalty walk algorithm,[2] path energy minimization,[3] conjugate peak refinement,[4] and targeted molecular dynamics[5]) and those that require no target structure. Of the algorithms that require no target structure, essential dynamics sampling,[6] principal component restraint MD[7] and conformational flooding[8] all analyze an initial MD simulation using an essential dynamics analysis and then perform an MD simulation modified to encourage the system to move in the essential modes. The generalized-ensemble methods[9] (multicanonical procedures, simulated tempering, and replica-exchange) have also recently been demonstrated to yield significantly enhanced sampling in protein systems but, most importantly, give populations consistent with the Boltzmann distribution.

An alternative procedure for probing conformational change in proteins is digitally filtered molecular dynamics[10] (DFMD), a development of selectively enhanced molecular dynamics[11] (SEMD). In DFMD, specially designed digital filters are applied in the time domain to the atomic velocities of an evolving simulation trajectory to selectively enhance or suppress vibrational motion based solely on vibrational frequency. By designing the digital filter to amplify low-frequency motion, conformational change may be enhanced. In this paper, the reversible digitally filtered molecular dynamics (RDFMD) method is presented. RDFMD modifies the DFMD algorithm to improve its control and performance, making it more suited to enhancing conformational change in protein simulations in which rapid energy dissipation is a problem.

The theory of RDFMD will be presented in this paper, followed by illustrative applications of the method to alanine dipeptide (gas-phase and solvated) and the pentapeptide Tyr-Pro-Gly-Asp-Val.

2. Theory

Both DFMD[10] and RDFMD apply nonrecursive digital filters to atomic velocity sets taken from MD simulations. Digital filters are commonly applied to sampled data series, such as a sound sample, which have a time index. A digital filter is no more than a list of numbers (coefficients), but the coefficients are carefully chosen using a design algorithm such that when the filter is applied to the data a desired frequency response is achieved.[12] The "frequency response" may often simply be described in words as, for instance, "amplify frequencies 0−50 Hz by 2 times" or "remove everything above 200 Hz". An example of a desired frequency response, the actual frequency response of a filter designed using the *fircls* function in MATLAB,[13] and a plot of the filter coefficients are shown in Figure 1. The greater the number of coefficients used in the filter design, the closer the actual response will be to the desired response. We have found that filters with 1001 coefficients are often sufficient.

To apply a nonrecursive digital filter to a data set, each filter coefficient, c_i, is multiplied by the corresponding data point and

* To whom correspondence should be addressed. E-mail: J.W.Essex@soton.ac.uk.

10.1021/jp026456f CCC: $25.00
Published on Web 02/07/2003

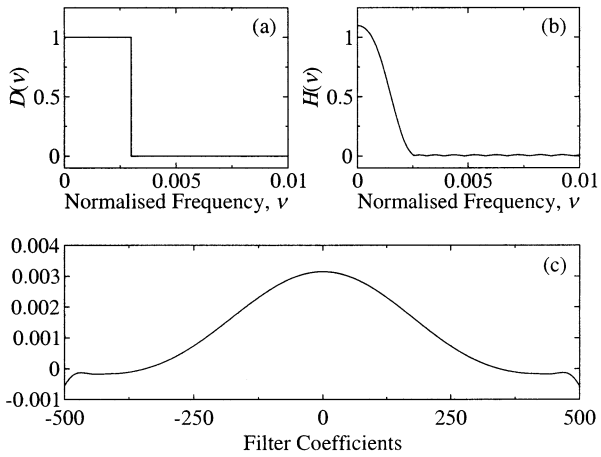

Figure 1. (a) Desired filter amplitude response, $\mathscr{D}(\nu)$; (b) the actual filter amplitude response of the designed filter, $\mathscr{H}(\nu)$, for 1001 coefficients; (c) the filter coefficients.

the products are summed to give the filter output:

$$y_k = \sum_{i=-m}^{m} c_i x_{k-i} \tag{1}$$

The filter's $2m + 1$ coefficients are numbered from $-m$ to m and may be applied to any point, k, in the data series, x. The data series is numbered from 0.

A digital filter will affect the amplitude and phase of every frequency present in the data set. Using filter design algorithms, we may control the filter's effect on the amplitudes, but simultaneously controlling the amplitude and phase is difficult. The solution adopted here (and in many digital filter applications) is to use a "linear phase filter" in which the coefficients are symmetrical, e.g., $c_{-i} = c_i$. The relative phase of the middle input point, x_k, and the filter output, y_k, is zero for this class of filter.

The basic technique of DFMD is design a filter for the particular application and run a normal MD simulation for the same number of steps as the number of coefficients in the filter, while storing the velocities of the atoms at each step in a buffer. The system state (atomic coordinates, forces, etc.) must also be stored at the time step corresponding to the midpoint of the filter buffer. When the buffer is full, the filter is applied to the stored velocities as follows:

$$\mathbf{v}'_{n,t} = \sum_{i=-m}^{m} c_i \mathbf{v}_{n,t-i} \tag{2}$$

where n is the index of the atom and $\mathbf{v}_{n,t}$ is the velocity vector for atom n at time step t. The filter output, $\mathbf{v}'$, is a new set of atomic velocities. The new velocity set is in phase with the midpoint of the filter buffer, and so to continue with the MD simulation, the previously stored system state from the midpoint is restored. Molecular dynamics can then continue with the new, filtered velocities.

This technique works effectively in simple gas-phase simulations where the atomic velocities are only causing molecular vibrations.[10] In the condensed phase, the velocities cause molecular vibration, rotation, and translation. As the method is only intended to target intramolecular vibration (and, through that, molecular conformational change), the DFMD algorithm is modified such that the velocity components responsible for molecular translation and rotation are removed from the stored velocity buffer. The filter is applied to the remaining "internal velocities" and the filter output is a set of internal velocities modified according to the filter's frequency response. To continue the MD simulation, these new internal velocities are added to the translational and rotational velocities from the stored central system state.

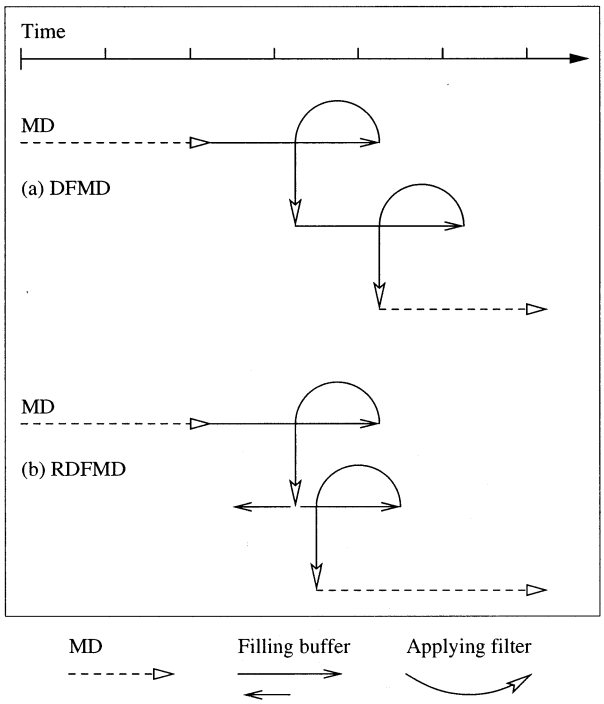

Figure 2. DFMD and RDFMD methods: (a) applying the DFMD method twice, with no pause between; (b) two applications of the RDFMD method, moving the center of the filter slightly forward in time.

The main difference between the previously published DFMD method and the RDFMD approach reported here lies in how the methods apply the filter for the second and subsequent occasions. In DFMD, a "multiple pulse" technique is used to apply the filter several times to a single extended filter buffer, but apart from that, once the filter has been applied, the buffer must be refilled from the start before the filter can be applied again (see Figure 2a). We have found that once energy has been introduced into the low-frequency vibrations of a condensed phase simulation it dissipates rapidly. In the simulation of the solvated pentapeptide presented below, the half-life of the internal kinetic energy decay (calculated from the internal velocities) after applying a $0-25\ \mathrm{cm}^{-1} \times 10$ amplifying filter was found to be approximately 20 time steps (40 fs). If, in DFMD, we start storing velocities for a second filter application immediately after the first application, the decay in the internal kinetic energy will be such that applying the filter to this buffer will be effectively no different to the first application; that is, the extra energy added in the first application will be lost. To cause conformational change using DFMD therefore, all of the necessary energy must be imparted to the system in a single DFMD application in which the velocities being filtered are obtained solely from sampling the bottom of the potential well. If the shape of the potential surface changes as the transition state is approached, then amplifying on the basis of these stored velocities will be less than optimum. However, by increasing the energy in the selected frequency range in a gradual manner and filtering based on these gradually amplified velocities, the MD system is able to explore higher potential energy regions before conformational change occurs. This has the advantage that the final conformational change will be more realistic than

the motion caused by a sudden large increase in kinetic energy, as the system will have spent time sensing the shape of the potential energy surface as it approaches the transition. The RDFMD technique is an extension to the DFMD method which lets the second and subsequent filter applications be positioned anywhere in time relative to the first application. By moving the application point forward only slightly in time and by applying a small amplification filter, each small amplification may build on the previous filter applications and energy may be added in a gradual manner.

When a filter is applied, the coordinates and forces are restored from the center of the filter buffer. In RDFMD, the position of the center of the filter buffer for the second and subsequent applications is specified by the user. This is achieved by filling the new buffer from MD simulations run both forward and backward in time after the first filter application. Running the simulation backward in time is achieved by simply changing the sign of the time step. Figure 2b shows a typical example of the RDFMD method. Normal MD is used first, followed by a period during which the filter buffer is filled. The filter is then applied, taking the coordinate set from the midpoint of the filter buffer. Up to this point, RDFMD is exactly the same as DFMD. Next, two simulations are run, both continuing from the initial filter application: one simulation proceeds forward in time, whereas the second simulation changes the sign of the time step and goes backward in time. The filter buffer is refilled, with the first part of the buffer taken from the backward simulation and the rest of the buffer taken from the forward simulation. The filter is then applied in the usual way with the system state being restored from the center of the buffer. Normal MD or further filter applications may follow.

By varying the proportion of the new buffer taken from the backward simulation, one can choose the position of the new center point. For instance, if the filter buffer consisted of 8001 coefficients and simulations were performed both backward and forward for 4000 steps, then the center point of the new buffer would be in the same place as before. However, by simulating backward for 3990 steps and forward for 4010, the center point of the new buffer is moved 10 steps forward. The effect is to yield a full filter buffer from an amplified trajectory but with a choice of filter buffer center point. By choosing the center point of the new filter buffer to be near the center point of the old buffer, the filter application is able to build on the energy added to the system by previous applications, and energy dissipation effects can be minimized.

To simulate backward in time, a time-reversible integrator is required. The velocity Verlet[14] is such an integrator. The velocity Verlet calculates and stores the positions and velocities at each time step (rather than holding the velocities half a time step out of phase, as in the leapfrog Verlet, or not at all, as in the original Verlet). This means that it is trivial to reverse the integrator by changing the sign of either the time step or the velocities.

To apply the RDFMD method to an MD simulation, the following procedure is recommended:

1. Run an MD simulation and analyze the motion using Fourier transform methods[10] or the Hilbert−Huang transform[15,16] (HHT). This will allow for the identification of the characteristic frequencies of the vibrations to be modified.

2. From the analysis, choose the desired frequency response of the digital filter. If the filter is to enhance conformational change, it will commonly amplify a low-frequency range and leave higher frequencies untouched.

3. Use a tool such as MATLAB[13] to calculate the digital filter coefficients, using as few coefficients as possible, while still having an acceptable frequency response.

4. Using normal MD, generate a variety of start points for the RDFMD simulations.

5. From the starts points, run normal MD to fill the filter buffer. Apply a filter to produce a large amplification in the chosen frequency range and calculate the half-life of the internal kinetic energy decay.

6. Run RDFMD from the start points, introducing energy gradually and leaving a half-life delay between filter applications. Monitor the behavior of the system using Fourier and HHT methods.

2.1. Simulation Analysis. An atom in an MD simulation vibrates with many frequencies. A plot of a component of the atom's coordinate or velocity will in general show a complicated waveform because of the superposition of these frequencies. It is useful to analyze a molecular dynamics trajectory to find out what frequencies of motion are present. One method of doing this is to calculate the spectral density.

The spectral density is calculated using a Fourier transform of the atomic velocity or coordinate components.[17−19] This has the advantage that none of the harmonic approximations associated with normal-mode analysis are used and that the spectra obtained are based on entire MD trajectories. The spectral density, $g(\nu)$, can be thought of as the simulation equivalent of an IR vibrational spectrum. It shows the relative amount of energy (or density of states) in each frequency, ν Hz. The integral of $g(\nu)$ is theoretically the total number of degrees of freedom in the system.

For n particles with masses m_n, oscillating at temperature T K in three dimensions, the formula for the $g(\nu)$ in terms of the velocities is as follows:

$$g(\nu) = \sum_n g_n(\nu) = \sum_n \frac{1}{kT} m_n \left(\int_{-\infty}^{\infty} \dot{x}_n(t) e^{-2\pi i \nu t} dt \right)^2 \qquad (3)$$

where k is the Boltzmann constant and the sum across the x, y, and z dimensions is implicit.

A variation of the spectral density may be used to focus on the motion in an internal coordinate, such as a single bond or dihedral. To do this, the internal coordinate must first be calculated as a function of time from the stored Cartesian coordinate trajectory. The spectral density eq 3 is not appropriate in this situation because it requires the mass of the oscillator. For an oscillating diatomic, the reduced mass may be used, but for any larger system, the reduced mass equivalent is not known. However, for the case of a single internal coordinate trajectory, the mass merely scales the data in the y axis, and so it can be removed from the equation along with the other scaling factors. The spectral density equation for a single degree of freedom is therefore

$$g(\nu) = \left(\nu \int_{-\infty}^{\infty} x(t)\, e^{-2\pi i \nu t}\, dt \right)^2 \qquad (4)$$

In general, the magnitude of the peaks in a spectrum calculated from this equation cannot be compared quantitatively to another spectrum because the mass term and the other scale factors have been removed. Relative peak heights within a single spectrum can, however, safely be compared.

In some situations, it is most useful to look at the relative amplitudes of the various frequency vibrations present in an internal degree of freedom, rather than the relative energies. In

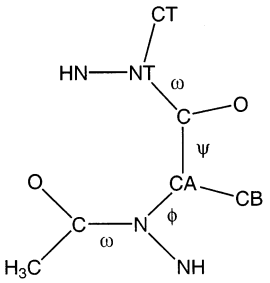

Figure 3. United-atom alanine dipeptide showing the ϕ, ψ, and ω backbone dihedral angles.

this case, the basic Fourier transform is taken, without the additional frequency scaling.

An alternative trajectory analysis method is the recently developed HHT[15] which can provide detailed information on how the frequency spectrum varies with time. The HHT has been successfully applied to the analysis of MD trajectories, including some of the simulations presented here. This work will be presented elsewhere.[16]

3. Applications

The application of RDFMD to three systems is presented: to gas-phase and liquid-phase alanine dipeptide, where many good conformational transitions are induced, and selectivity for the type of transition is achieved, and to the pentapeptide Tyr-Pro-Gly-Asp-Val (YPGDV), where a protocol is developed to induce and analyze conformational change in a system where the potential surface is not known.

The alanine dipeptide MD simulations were performed using a modified version of DLPROTEIN.[20]

3.1. Alanine Dipeptide. Alanine dipeptide (or *N*-acetyl-L-alanine-*N*-methylamide) was chosen because it is quite complex, with 12 united atoms and two distinct and variable dihedral angles, and yet sufficiently simple for a detailed and complete analysis to be performed. It is also a peptide and therefore has the conformational properties of proteins, the ultimate target of this work. Figure 3 shows united-atom alanine dipeptide. There have been many simulation studies of alanine dipeptide; these include the self-penalty walk method,[2] the Olender and Elber paper[21] on long time step methods, the Wu and Wang paper[22] on self-guided molecular dynamics, and the leap-dynamics method of Kleinjung et al.[23] Others have studied alanine dipeptide in solution and used various methods for calculating potentials of mean force for its conformations[24−28] and a conformational probability map.[29] Other studies of conformational transition paths have also been performed.[30,31]

3.1.1. Potential Energy Surface. The major conformational transitions in alanine dipeptide are changes in the ϕ and ψ backbone dihedral angles (see Figure 3). In common with other peptides, the ω backbone dihedral angles remain fairly static. A picture of the potential energy surface is necessary in order to understand any conformational change. Figure 4 shows the potential energy surface as calculated using BOSS[32] and various Perl scripts. The united-atom OPLS force field,[33] provided in BOSS, was employed.

3.1.2. Inducing Conformational Change. For the molecular dynamics simulations, alanine dipeptide was initially placed in minimum B (see Figure 4). Minimum B is not the lowest energy minimum, but it is the deepest, in that the potential energy barrier to reach another minimum is highest. The force field parameters used in the potential surface calculation were manually translated into the DLPROTEIN program format. All bonds were constrained by SHAKE,[34] and a 2 fs time step was

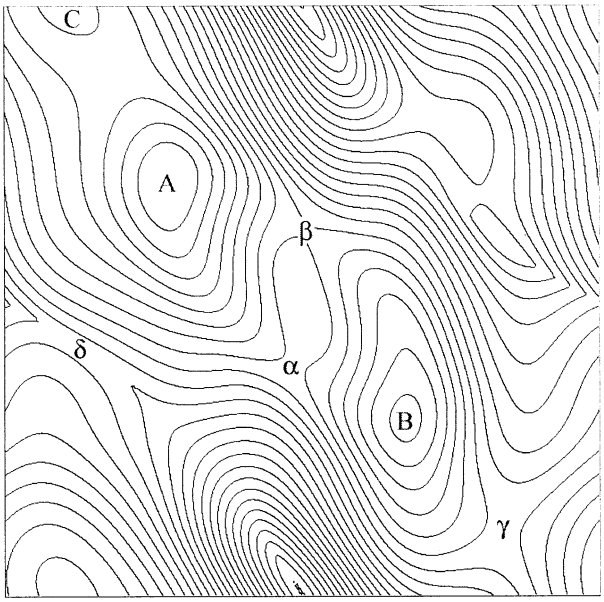

Figure 4. Adiabatic potential energy surface of alanine dipeptide with ϕ on the *x* axis and ψ on the *y* axis. A, B, and C are three minima and α, β, γ. and δ are transition points. Contours are shown every 1 kcal mol^{-1} (approximately 4 kJ mol^{-1}).

employed. The initial simulation of the single alanine dipeptide molecule was run for 20 000 steps (or 40 ps). The ensemble was the NVE microcanonical ensemble, and the initial temperature was 293 K. The simulation was then run for a further 100 000 steps, with restart points saved every 20 000 steps. During these simulations the dipeptide remained in minimum B. The five restart points provided five different starting points for the RDFMD experiments. Each RDFMD simulation was started from each of these five start points, to ensure that the results were reproducible and not a result of a particular starting conformation.

To induce conformational change using a digital filter, it is necessary to identify the target frequencies. Figure 5 shows the spectral density of the first 40 ps of the second simulation and the amplitude spectra obtained from the ϕ and ψ dihedral angle trajectories. The largest amplitude low-frequency peak is the ψ dihedral peak at 50 cm^{-1}. This peak was chosen as the initial target for amplification.

To target the ψ dihedral angle, the filter shown as a solid line in Figure 6 was designed in MATLAB.[13] The design command used was fircls(2000, [0 0.0054 0.0066 1], [1 2 1], [1.01 3 1.01], [0.99 2 0.99], "text"). This means that the filter has 2001 coefficients and has transitions at 45 and 55 cm^{-1}, moving from a response of 1 to 2 to 1. The response of 1 is constrained to be between 0.99 and 1.01, and the amplifying response is constrained between 2 and 3. The small number of coefficients used means that the constraints cannot be perfectly satisfied and the filter amplifies by at most 1.84. The filter response is a long way from the ideal response and is sloped rather than square, but this does not matter because the target frequency is also not precisely defined.

When attempting to use the 50 cm^{-1} amplifying filter to produce a transition, it was found that after a few filter applications the 50 cm^{-1} filter did not introduce any more energy into the system but that the 40 cm^{-1} amplifying filter shown as a dashed line in Figure 6 could. The design command for the 40 cm^{-1} filter was the same as the 50 cm^{-1} filter but with transitions at 35 and 45 cm^{-1}. It was postulated that the reason that the 50 cm^{-1} filter stopped working and the 40 cm^{-1} filter

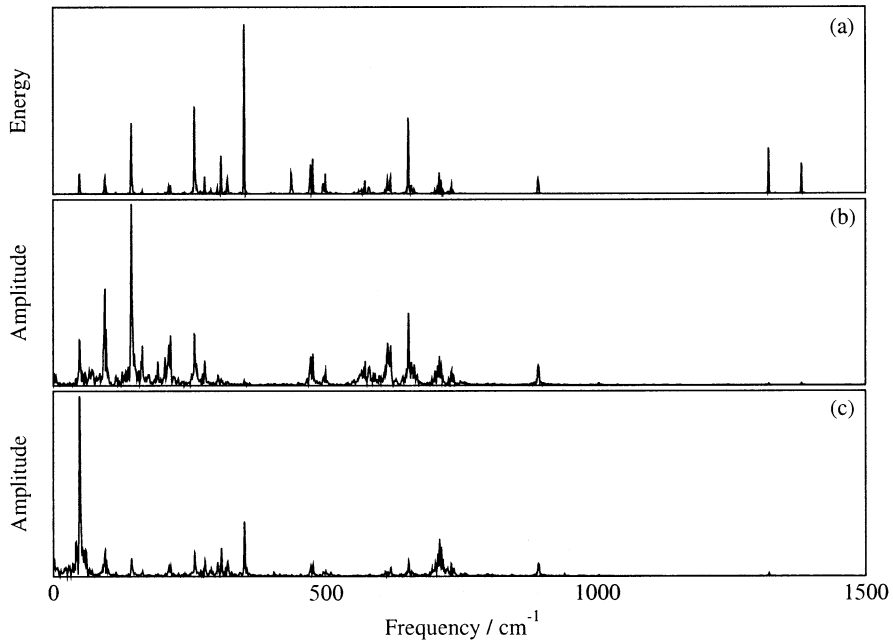

Figure 5. Alanine dipeptide: (a) the spectral density of a 40 ps MD simulation; (b) the amplitude spectrum of the ϕ dihedral angle; (c) the amplitude spectrum of the ψ dihedral angle. All the *y* axes are to different scales.

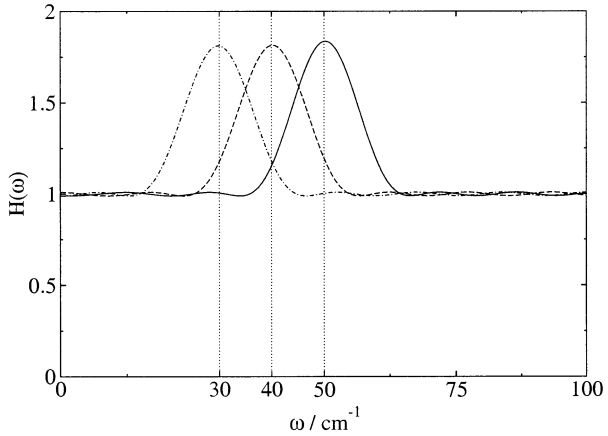

Figure 6. Three filters designed in MATLAB for amplifying the ψ backbone dihedral of alanine dipeptide. The filter depicted as a solid line targets 50 cm^{-1}, the dashed filter targets 40 cm^{-1}, and the dot−dash filter targets 30 cm^{-1}. All filters use 2001 coefficients.

TABLE 1: Average Energies after Each Application of the 50 cm^{-1} Amplifying Filter

filter application no.	energy/kJ mol^{-1}		
	total	kinetic	potential
	−147.0	11.5	−158.5
1	−147.3	11.4	−158.7
2	−145.5	12.0	−157.5
3	−145.0	12.2	−157.2
4	−144.9	12.3	−157.2
5	−144.9	12.3	−157.2

was able to add energy was that the frequency of the target dihedral had shifted. The investigation of the frequency shifting will be presented first, followed by the experiments to cause transitions.

To investigate the frequency shift, one of the start points was chosen, and the 50 cm^{-1} filter was applied five times with a zero step delay between applications. The zero step delay ensures that any effect is caused by the nature of the filter applied rather than by the time of application. Table 1 lists the average energies for each 2001 step simulation. The table shows

TABLE 2: Average Energies after Each Application of the 40 cm^{-1} Amplifying Filter

filter application no.	energy/kJ mol^{-1}		
	total	kinetic	potential
	−145.5	12.0	−157.5
1	−138.4	15.4	−153.8
2	−129.0	19.5	−148.5
3	−120.5	25.9	−146.4

a small amount of energy being added by the first four applications but no change after the fifth filter application.

Continuing from the second application of the 50 cm^{-1} filter, the 40 cm^{-1} amplifying filter was applied three times. The resulting average energies are listed in Table 2. The energies quickly increase with the 40 cm^{-1} filter, and after the third application, a conformational transition is produced via transition state γ. These simulations are a clear example of an important motion changing frequency as energy is added slowly.

The protocol used to cause conformational change was therefore as follows:

1. Apply the 50 cm^{-1} targeting filter with a pause of 15 steps between applications until it is no longer effective.

2. Continue from the last effective application with the 40 cm^{-1} targeting filter until it is no longer effective or conformational change has been caused.

3. Continue from the last effective application with the 30 cm^{-1} targeting filter until it is no longer effective or conformational change has been caused.

The 30 cm^{-1} targeting filter is also shown in Figure 6. Its design equation is the same as the other two filters except that the transition boundaries are at 25 and 35 cm^{-1}. The delay of 15 steps was chosen to allow the midpoint of the filter application to move each time. This is desirable because the midpoint of the filter application may be an unfortunate conformation with high potential energy in the mode being targeted. In this worst case, the filter will do very little, but by moving the application point slightly each time, subsequent applications will do more. Having the midpoint move slightly rather than a great deal means that these simulations are more

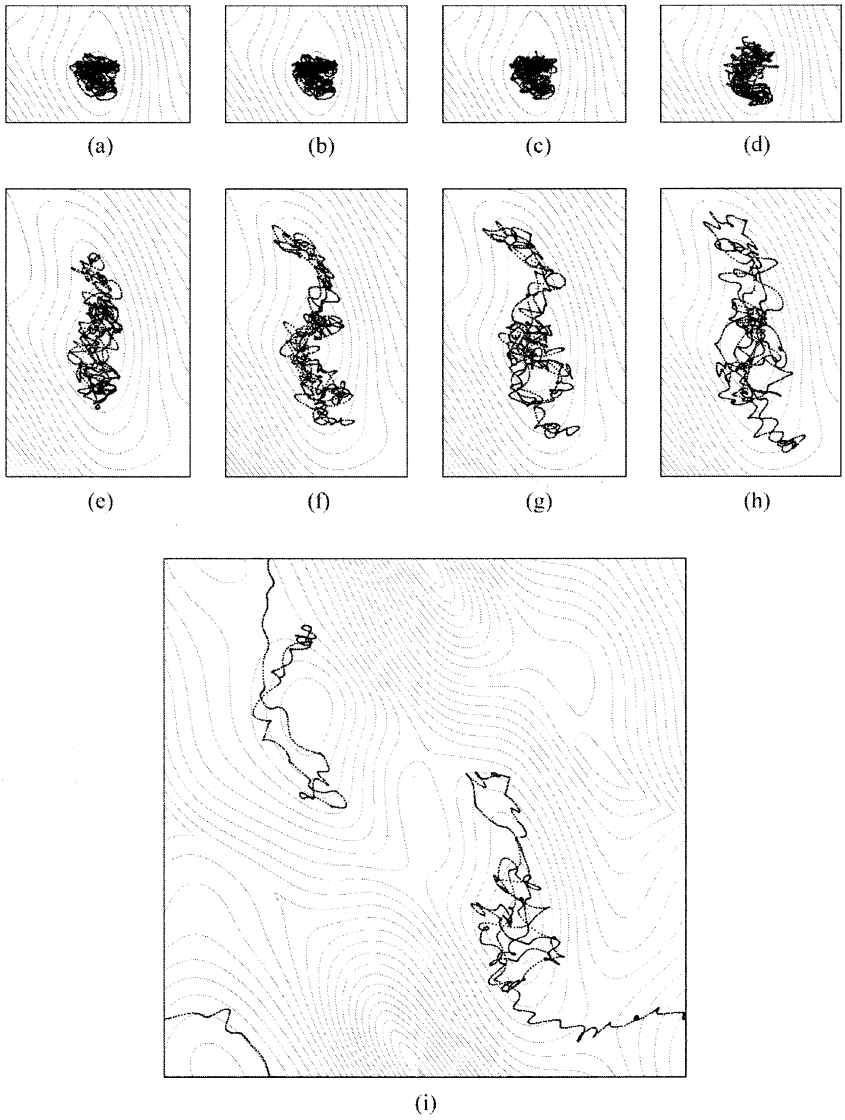

Figure 7. $\phi-\psi$ trajectory of alanine dipeptide resulting from RDFMD filter applications targeting the ψ dihedral angle. All parts show ϕ on the x axis and ψ on the y axis. Parts a−h show just small portions of the surface around minimum B. Part i shows the whole surface from −180 ° to +180 ° in both axes. Parts a−e show the result of successive applications of the 50 cm^{-1} targeting filter, and parts f−i result from continuing the sequence with the 40 cm^{-1} targeting filter.

TABLE 3: Number of Filter Applications Needed to Produce Conformational Change in Alanine Dipeptide[a]

start point	number of applications of filter			
	50 cm^{-1}	40 cm^{-1}	30 cm^{-1}	total
1	5	4		9
2	3	4		7
3	18...			>18
4	9	3		12
5	6	3		9
1	5		1	6
2	3		3	6

[a] No conformational change was found in the simulations beginning with start point 3.

similar to solution-phase simulations where energy dissipation becomes important.

The protocol given above was applied to the five start points. Table 3 lists the number of applications of each filter needed to cause conformational change. In no cases was it necessary to use the 30 cm^{-1} targeting filter, but a second set of simulations were run from each of the start points 1 and 2 in which the 30 cm^{-1} filter was used directly after the 50 cm^{-1} targeting filter. These two sets of simulations, listed at the bottom of Table 3, required fewer filter pulses than the corresponding simulations that used the 40 cm^{-1} filter, suggesting that the frequency of the dihedral motion has shifted closer to 30 cm^{-1} than 40 cm^{-1} in at least these cases. The simulation beginning with start point 3 behaved differently to the others. Even after 18 applications of the 50 cm^{-1} targeting filter, the dihedral motion was still only increasing slightly. Undoubtedly, conformational change could have been achieved by switching to one of the lower frequency filters but this was an interesting result in itself.

Figure 7 shows the $\phi-\psi$ trajectory from start point number 1, using the 50 and 40 cm^{-1} filters. The final transition is from minimum B to A via transition state γ. The transitions from start points 2, 4, and 5 were very similar. From this figure, it is obvious how the gradual addition of kinetic energy is resulting in the system sampling the potential energy surface more completely.

Targeting the ψ backbone dihedral angle is clearly an effective way of promoting a conformational transition from B to A. Is it possible to cause conformational change while

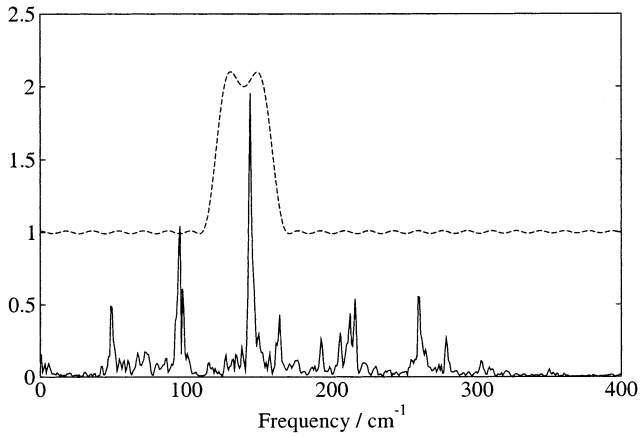

Figure 8. Solid line is the low-frequency part of the amplitude spectrum obtained from a 40 ps ϕ dihedral angle trajectory. The dashed line is the frequency response of the filter designed to target the ϕ dihedral. The data in the dihedral angle spectrum has been scaled in the *y*-axis to fit on the same graph as the filter response.

targeting the ϕ angle though? Figure 8 shows the low-frequency part of Figure 5b which is the amplitude spectrum obtained from a ϕ angle trajectory. Overlaid on this is the filter designed to preferentially target the ϕ angle. The matlab design command for this filter was fircls(2000, [0 0.0144 0.0192 1], [1 2 1], [1.01 3 1.01], [0.99 2 0.99], "text") which is the same as the previous filters used on alanine dipeptide but with transitions at 120 and 160 cm^{-1}.

Start point number 5 was chosen for this part of the study. The filter was used with a delay of 15 time steps between applications. Eight filter applications were necessary to produce conformational change, and though the transition was once again via transition point γ, the trajectory before the transition was very different to those produced by the filters targeting ψ. The trajectory immediately before the final filter application showed the ϕ angle with a larger range of motion than the ψ angle—contrary to what would be expected from the shape of the potential energy surface although consistent with the digital filter being applied. This result shows once again the specificity of the method.

3.1.3. Summary. The study of gas-phase alanine dipeptide has shown three things:

1. The frequency of a target motion can change as energy is added to the system. The RDFMD technique can adapt to these changes in frequency.

2. RDFMD can be used to produce conformational change in this system from a variety of start points.

3. By using different filters, it is possible to target either the ϕ or ψ dihedral angles preferentially, and that the nature of the sampling of the underlying potential is affected by this choice.

3.2. Solvated Alanine Dipeptide. To examine the effect of energy dissipation in the context of RDFMD, solvated alanine dipeptide was examined.

Water was unsuitable as a solvent as it is too polar and changes the potential energy surface. Chloroform ($CHCl_3$) interacts with the dipeptide sufficiently weakly so that the positions of the potential minima remain the same on moving from the gas phase to the solvated system. The intermolecular potential for chloroform was the default BOSS potential.[35] The equilibrium bond lengths and angles were also taken from BOSS. The valence angle potential for chloroform was taken from a model of carbon tetrachloride.[36] The system was set up by solvating the dipeptide in a cubic box of side 33 Å containing 310 chloroform molecules using BOSS.[32] A 1 500 000 step constant volume Monte Carlo simulation was performed to remove any bad interactions. For the subsequent MD, the SPME parameters were determined for 8 Å cutoffs. SHAKE was used to constrain all bonds, and a 2 fs time step was employed. A 100 000 step MD simulation was performed in the NPT (isobaric−isothermal) ensemble at 220 K and 1 atm pressure using the Melchionna[37] adaptation of the Hoover barostat and thermostat. A low temperature was used to prevent the dipeptide from spontaneously changing conformation; 220 K is 10 K higher than the freezing point of chloroform. During the 200 ps simulation, the temperature and pressure stabilized and the dipeptide remained in minimum B. Furthermore, all transition states and minima observed during the subsequent RDFMD simulations matched the adiabatic potential energy surface, supporting the use of this surface to highlight conformational change events.

3.2.1. Filter Design. The data used to determine the design of the filter was obtained from a 33 000 step NVE simulation restarted from the 200 ps NPT simulation above. A total of 33 000 steps gives a frequency resolution of 0.5 cm^{-1} which is more than sufficient. The amplitude spectra of the ϕ and ψ dihedral trajectories showed that the ϕ dihedral angle has large amplitude motion across a broad range of frequencies, whereas the large amplitude motion in the ψ dihedral is almost completely confined to the 0−100 cm^{-1} region.

To examine the distribution of the motion with frequency more closely, the trajectories of all of the internal degrees of freedom (valence angles and dihedrals) were calculated from the Cartesian coordinates. There are 15 valence angles and four sets of four dihedral angles. For instance, the ψ dihedral is generally defined to be the dihedral angle made by the four backbone atoms (C−N−CA−C in this case), but this dihedral makes a set of four along with the other three dihedrals sharing the same two central atoms (C−N−CA−CB, HN−N−CA−C, and HN−N−CA−CB). The four dihedral angles in a set can be expected to be closely related.

The manner in which the standard deviation of each internal degree of freedom trajectory changes as the high frequency components of the motion are removed will help show the frequency with which each degree of freedom moves. To do this, each trajectory initially has its mean subtracted. The trajectories are then Fourier transformed into the frequency domain, and all data above a cutoff frequency are set to zero. The signals are then back-transformed to the time domain, and their standard deviations calculated. The standard deviations are then measured, percentage-wise, against the standard deviations of the original signals. Nine frequency cutoffs were chosen to lie (as far as possible) between major peaks in the spectral density, so as to provide information on the type of motion represented by each peak or region.

Figure 9 plots the percentage of the original standard deviation for each of the 31 degrees of freedom and each of the nine frequency cutoffs. The percentage standard deviation for the 13 of the 15 valence angles is less than 25% by 400 cm^{-1}. This shows that most of the motion in the valence angles is at frequencies greater than 400 cm^{-1}. The set of four ψ dihedrals are almost indistinguishable in their attenuation and have greater than 50% standard deviation even with the 25 cm^{-1} cutoff, demonstrating that a large proportion of the motion in the ψ dihedral is at frequencies less than 25 cm^{-1}. The next highest signals at 25 cm^{-1} are, surprisingly, the dihedrals HN−NT−C−CA and HN−NT−C−O. These dihedrals are members of the ω set next to the ψ dihedral (see Figure 3). They have motion

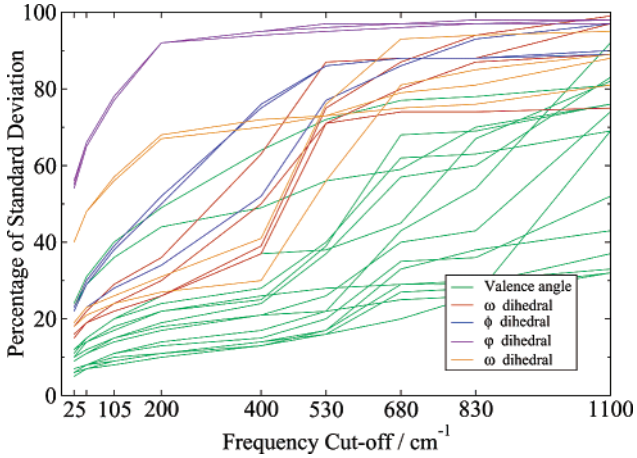

Figure 9. Each point in the plot corresponds to a particular degree of freedom and a particular frequency cutoff. The chosen cutoffs are marked on the *x* axis, including a cutoff at 50 cm^{-1}. The standard deviation of the original signal is compared with the standard deviation of the signal after passing it through a frequency filter with a high-frequency cutoff. This gives the percentage of standard deviation plotted on the *y* axis.

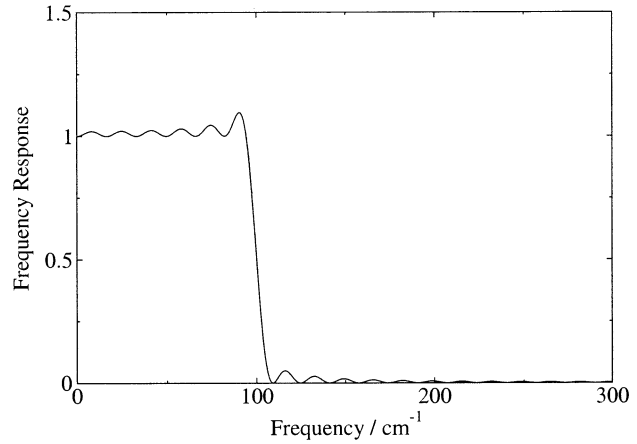

Figure 10. MATLAB design command for this filter is fircls(2000, [0 0.0120 1], [1 0], [1.1 0.05], [1 0], "text"). It has 2001 coefficients and a transition from 1 to 0 at 100 cm^{-1}. The response is constrained to lie within 1−1.1 and 0−0.05.

at this low frequency because of a small deviation in ψ away from the minimum, approximately 30 000 steps into the simulation. The motion was transferred into the neighboring ω dihedral and caused the hydrogen atom to vibrate at a similar low frequency. The four dihedrals in the ϕ set have around 20% standard deviation by the 25 cm^{-1} cutoff point. This is consistent with the earlier analysis that the energy in the ϕ dihedral is more dispersed than the ψ dihedral. The two valence angles that have significantly higher percentage standard deviations than the others are N−CA−C and CB−CA−C. These angles are involved in the ψ dihedral motion.

Considering this analysis, it was decided that the best filters for inducing conformational change would target only the low-frequency region. A filter targeting 0−100 cm^{-1} will capture approximately 75% of the ψ motion and almost 40% of the ϕ motion (according to the standard deviation) while not affecting the other degrees of freedom significantly. All of the filters used in the rest of this section are derived from the filter shown in Figure 10 by scaling and shifting the coefficients. To create a filter which amplifies 0−100 cm^{-1} by three and the rest by one, the filter of Figure 10 (which has responses of one and zero in the two regions) is multiplied by two (to yield a filter with responses of two and zero) and one is added to its middle coefficient to raise the magnitude of the whole frequency response by one and yield the required filter.

3.2.2. Energy Dissipation. Before any attempt is made to induce conformational change in the system, several start points must be generated and a sensible delay between filter applications must be determined. Ten start points were generated by running successive 8 ps NVE simulations.

To find a good value for the time step delay between filter applications, the rate of energy dissipation from the internal velocities of the alanine dipeptide was investigated (where "internal velocities" refers to the atomic velocities with the rotational and translational components removed, as used to fill the filter buffer). To do this, a filter amplifying 0−100 cm^{-1} by 20 times was applied to five start points. The kinetic energy of the internal velocities was calculated at each step, and first-order decay curves were fitted to the resulting data. The five start points provide 10 possible energy decay measurements by taking data from both forward and backward simulations. The third start point was not affected by the filter application, and so an exponential decay curve could not sensibly be fitted. The remaining eight half-life measurements were 11, 11, 12, 15, 18, 21, 21, and 30 time steps. In a condensed-phase simulation such as this, we therefore need a delay that is long enough to allow the filter midpoint to move but short enough such that the energy introduced by one filter application has not dissipated before the time of the following filter application. Fifteen time steps were used in the gas-phase simulations, and fifteen were also chosen for the following solution-phase simulations.

3.2.3. Inducing Conformational Change. Conformational change was produced in all 10 test cases using the following protocol:

1. Apply a 0−100 $cm^{-1} \times 2$ filter with a 15 time step delay until conformational change is observed. Stop if the conformational change is acceptable.

2. Take a point a few filter applications before conformational change was caused and apply a 0−100 $cm^{-1} \times 1.5$ filter until conformational change is observed.

The reason for the two-step protocol is that a $\times 2$ filter was found, in some cases, to cause transitions in which the dihedrals were moving quickly or via high energy points in the potential energy surface. By switching to a $\times 1.5$ filter a few filter applications before the conformational change was observed, the quality of the transition may be improved.

The results of applying this protocol to the 10 start points are listed in Table 4. It was possible to produce conformational change in 9 of the 10 start points. Of the 9 successful cases, the paths taken included all possible transition points (α, β, and γ), and the dipeptide finished in both minimum C and minimum A. It was not possible with this protocol to produce reasonable conformational change from start point four.

3.2.4. Comparison with a Heating Pulse. As a further validation of the technique, the transition trajectories of the 10 start points were compared with trajectories resulting from single-pulse filter applications, where the frequency response of the filter was the same for all frequencies. Application of one of these filters scales all frequencies to the same degree and can be called a "heating pulse". For each of the 10 start points, the mean total energy of the best transition was measured. A heating filter was designed (by trial and error) to reproduce this total energy in a single application. Each heating pulse was tuned to give at least the same energy as the best transition and no more than 50 kJ mol^{-1} (approximately 1% of the total)

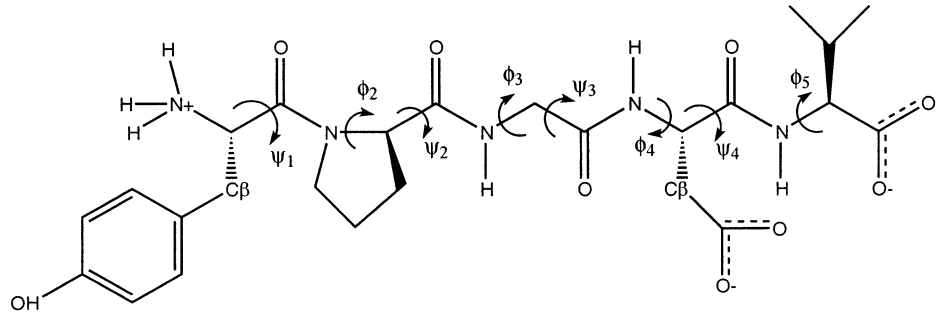

Figure 11. Tyr-Pro-Gly-Asp-Val (or YPGDV). The four ϕ and four ψ dihedral angles are shown (numbered according to residue).

TABLE 4: Number of Filter Applications Needed to Produce Conformational Change in Alanine Dipeptide in Chloroform[a]

start point	filter applications			transition point	final minimum
	× 2	× 1.5	total		
1	6		6	γ	C
1	5	2	7	γ	C
2	10		10	γ	C
3	13		13	β	A
4	5		5		A
4	2	6	8		B
5	15		15	γ	C
5	13	4	17	γ	C
6	9		9	γ	C
6	8	2	10	γ	C
7	8		8	γ	C
7	6	5	11	γ	C
8	4		4	β	A
9	8		8	γ	C
9	6	3	9	γ	C
10	5		5	α	A
10	4	1	5	α	A

[a] The transition point and minima labels refer to Figure 4.

higher. No transition were induced by the heating pulses, once again demonstrating the benefit of the frequency selective nature of the method.

3.2.5. Summary. The frequency spectrum of alanine dipeptide solvated in chloroform was studied by its spectral density, by the amplitude spectra of the ϕ and ψ angles, and by measuring the change in the motion of every internal degree of freedom as a series of high-frequency cutoffs were applied. This analysis led to the use of filters amplifying the $0-100$ cm^{-1} region for promoting conformational change. The half-life of the energy dissipation from the internal velocities of alanine dipeptide was measured, and a 15 time step delay between filter pulses was chosen as a result. A protocol using $\times 2$ filters followed by $\times 1.5$ filters was designed and applied to 10 start points. It was possible to produce good conformational transitions in all but one of the start points via three of the four saddle points. The application of a measured heating pulse to each start point produced no conformational change, demonstrating the advantage of the frequency selectivity of the digital filters.

3.3. Peptide YPGDV. The final and most complex system studied by RDFMD was the pentapeptide YPGDV (Tyr-Pro-Gly-Asp-Val) solvated in water. NOE data for this system were experimentally determined by Dyson et al.[38] in 1988. The *trans*-Proline form of the peptide (shown in Figure 11) was found to form a high population (approximately 50%) of reverse turns in water at 278 K. Tobias et al.[39] performed two 2.2 ns MD simulations of YPGDV at 300 K in 1991 using the CHARMM peptide parameters[40] and TIP3P water.[41] They started one simulation in an extended conformation and another simulation in a type II reverse turn conformation and found that the extended conformation folded and the folded conformation became extended. The two trajectories were further analyzed in 1993 by Karpen et al.[42] using the ART-2′ clustering algorithm, which is based on a self-organising neural network and is implemented in the CHARMM molecular mechanics program.[40]

Wu and Wang recently simulated YPGDV using normal MD and the SGMD method.[43] The simulations were performed in CHARMM using the all-atom CHARMM22 force field[44] and TIP3P water. A 2 ns MD simulation initiated from an extended conformation did not fold into a type II turn, whereas a 2 ns SGMD simulation started from the same extended conformation sampled more conformations, including a type II turn. The conformations sampled in the SGMD simulation were clustered according to Wu and Wang's own method and the conformation at the center of the largest cluster was used as the start point for a further 2 ns normal MD simulation, during which no conformational change was observed. The implication is that the conformation at the center of the largest cluster is in a very stable conformation. The method of NOE calculation reported in this paper has been used to analyze the MD and RDFMD simulations of the pentapeptide.

3.3.1. System Set-Up. The simulation system was constructed to be similar to that used by Wu and Wang.[43] An all-trans Z-matrix of YPGDV was generated by Pepz, part of the MCPRO[45] package. The default settings of $-70°$ for the ϕ angle in Pro and 180° for all of the other backbone dihedral angles causes a side-chain clash. This clash was removed by adjusting the two dihedral angles between the backbone and the tyrosine ring. MCPRO[45] was used to solvate the pentapeptide in TIP3P water. The backbone dihedral angles were fixed and MCPRO was used to make 300 000 NVT MC steps; this removed any bad interactions caused by the manner of solvation. For these simulations, the all-atom OPLS force field was used.[46] The resulting set of coordinates were visualized and a water molecule approximately 16 Å from the peptide was replace with a Na^+ counter-ion. The final system contained 805 water molecules and was converted into a format suitable for NAMD,[47] which was used for the remaining system equilibration and for the data production. NAMD was developed by the Theoretical Biophysics Group in the Beckman Institute for Advanced Science and Technology at the University of Illinois at Urbana-Champaign.

For the MD and RDFMD simulations, the all-atom CHARMM22 force field[44] was adopted for the peptide, together with the CHARMM implementation of the TIP3P water model. Wu and Wang used a residue-based cutoff with a nonbonded pair-list cut at 13 Å and a switching function applied between 8 and 12 Å. In the work presented here, the PME method[48] was used to calculate the long-range electrostatic interactions, using an interpolation order of 6 and 27 grid points in each

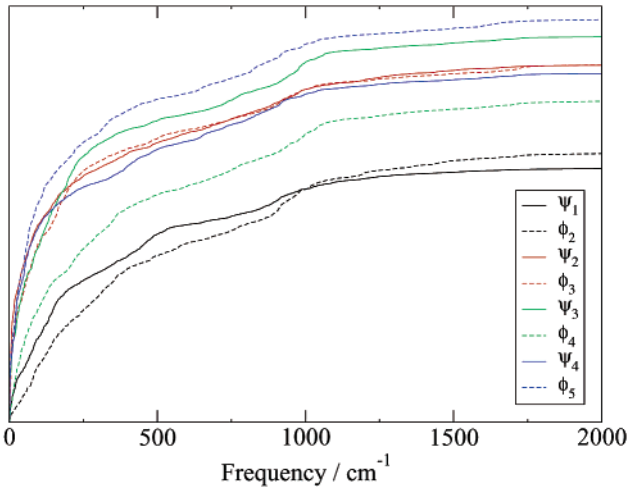

Figure 12. Cumulative sums of the amplitude spectra of the eight ϕ and ψ backbone dihedral angles of YPGDV. The quantitative value of the cumulative sum (on the *y*-axis) has no physical meaning. The graphs show the presence of large-amplitude low-frequency motion.

dimension. A switching function between 8 and 12 Å was applied to the Lennard Jones interactions, for consistency with the work of Wu and Wang. An atom-based nonbonded pairlist was cut at a distance of 13 Å for the production simulations and 15 Å for the minimization and equilibration phases. The system was minimized using the conjugate gradient line-search algorithm in the NAMD program;[47] initially, 12 000 steps of minimization were performed on the water molecules, followed by 4000 steps of minimization on the protein and counterion. A total of 6000 steps of unconstrained minimization were then performed.

The simulation system was gradually heated using a series of canonical simulations between 50 and 300 K, with a step size of 50 K. A total of 20 000 steps of molecular dynamics were performed at each temperature using a time step of 2 fs. Temperature was constrained using a Langevin Thermostat[49] with a damping parameter of 10 ps^{-1}. A further 80 000 steps of molecular dynamics were then performed at 300 K. Throughout the molecular dynamics simulations, SHAKE[34] was applied to all bonds containing hydrogen atoms, with a tolerance of 10^{-8} Å. A total of 500 000 time steps of equilibration in the isothermal isobaric (NPT) ensemble were then performed, using a Nosé-Hoover Langevin piston barostat[50] with a piston temperature of 300 K, a damping decay parameter of 200 fs, and an oscillation period of 400 fs. The thermostat parameters were unchanged.

A further 100 ps of constant NPT molecular dynamics were then performed, with looser thermostat and barostat parameters (1 ps^{-1} thermostat damping parameter, barostat damping decay of 300 fs, and piston oscillation period of 500 fs). The final coordinates and velocities from this simulation were then used for all the production simulations reported below. The final cubic equilibrated simulation system had cell dimensions of 28.9 Å.

3.3.2. Filter Design. To help decide what frequencies to target, a 16 678 step simulation in the NVE ensemble was performed. The spectral density of the peptide was not found to be helpful for the filter design. Instead, the amplitude spectra of the eight ϕ and ψ angles were calculated with 1 cm^{-1} resolution. The cumulative sum of the amplitudes with frequency is shown in Figure 12. Although the quantitative value of the cumulative sum has no physical meaning, the shape of the graphs show the presence of large-amplitude low-frequency motion. The dihedrals with the least motion are ψ_1 and ϕ_2, because they are constrained by the proline ring.

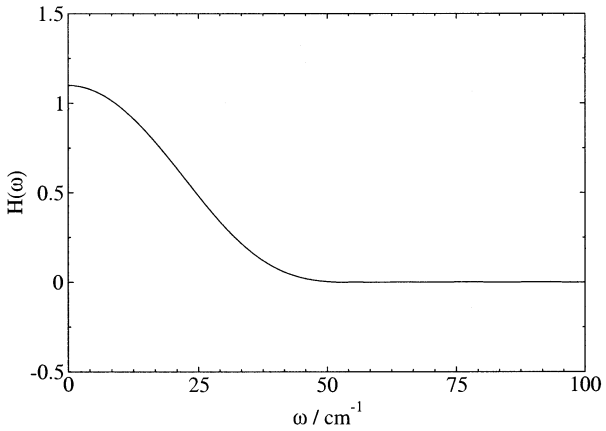

Figure 13. Frequency response of the filter designed for YPGDV. All filters used in the pentapeptide work are derived from this filter.

To target the dihedral motion while minimizing the effect on the other degrees of freedom, a filter designed for amplifying 0−25 cm^{-1} and using only 1001 coefficients was created in MATLAB. As with solvated alanine dipeptide, the filter was designed with frequency responses of 1 and 0, and all filters used in this section were derived from this one seed filter by multiplying the coefficients through by one less than the required amplification and then raising the whole frequency response by 1 by adding 1 to the middle coefficient. The filter, shown in Figure 13 has a very slow transition from the $\mathcal{H}(\omega) = 1$ region to the $\mathcal{H}(\omega) = 0$ region as a result of the relatively small number of coefficients used. By using a small number of coefficients in the design, the amount of data-collection required by the RDFMD steps is minimized, while a filter that generally enhances low-frequency motion is created. The MATLAB command for designing the seed filter is fircls(1000, [0 0.002998 1], [1 0], [1.1 0.001], [0−0.001], "text"). The boundary between the two regions (for a 2 fs time step) is at 25 cm^{-1}; the low-frequency region is constrained between 0 and 1.1, and the high-frequency region is tightly constrained between −0.001 and 0.001.

To determine the half-life of the energy dissipation in this system (and thus judge the size of the delay required between filter applications), five simulations from five start points were run. In each simulation, a 0−25 cm^{-1} × 10 amplifying filter was applied twice using a 15 time step delay (the 15 step delay was taken from the solvated alanine dipeptide work). The decay of the internal kinetic energy of the pentapeptide was plotted against time, and exponential decay curves were fitted to the data. The decay curves fitted to the data resulting from the second filter applications all had correlation coefficients greater than 0.93. The half-lives of these decay curves averaged to 20 time steps (with a variance of 6 time steps). A 20 time step delay was therefore used for the pentapeptide.

3.3.3. Inducing Conformational Change. In the SGMD simulation of YPGDV,[43] the self-guiding force was applied constantly for 2 ns, but it is not possible to apply the RDFMD method constantly. Instead, MD simulations in the NPT ensemble, alternating with RDFMD filter applications in the NVE ensemble have been performed.

Various RDFMD protocols were devised and tested. The protocol must gradually introduce frequency-targeted energy into the system to induce conformational change, but it is important not to put too much energy into the system and produce conformational change via high-energy pathways. The most successful protocol is described here.

An initial 20 ps NPT MD simulation is performed followed by alternating RDFMD and MD stages until 100 20 ps NPT simulations are complete (2 ns in total). In each RDFMD stage, as long as the internal temperature of the pentapeptide does not exceed 2000 K, the digital filter is applied 10 times (always in the NVE ensemble). The first of these filter applications is based on a buffer created by simulating for a further 1001 time steps after the NPT run. For the remaining filter applications, the buffer is created by simulating 520 steps forward in time, and 480 steps backward in time. These simulations are restarted from the previous filter output.

We switch from the NVE to the NPT ensemble in two cases:

1. The internal temperature of the pentapeptide (calculated using the same "internal velocities" as used by the filtering process) exceeds 2000 K immediately after a filter application.

2. The filter has been successfully applied for a total of 10 times.

To sample as much conformational change as possible, the next NPT simulation is restarted from the final frame of the last forward NVE run. However, if the first amplification exceeds the temperature cap, the NPT is restarted from the final frame of the preceding NPT simulation. In this manner, by adding together all of the NPT runs and excluding the NVE simulations, a 2 ns NPT trajectory is simulated. The choice of temperature cutoff is somewhat arbitrary. However, replica exchange simulations[9] are currently being performed to determine the most appropriate value for this temperature cutoff.

The analysis of the simulation performed using this protocol is presented below.

3.3.4. Results. In this section, the 2 ns NPT RDFMD trajectory is compared with the 2 ns SGMD trajectory and with a 4 ns MD simulation run in the NPT ensemble using the same starting point and force field as the RDFMD simulation. In the RDFMD simulation, the state of the system was saved to disk every 1 ps, whereas for the NPT MD simulations, the system coordinates were saved every 2 ps, to ensure that the same overall number of coordinate frames were analyzed. Of the 100 RDFMD cycles applied, 49 were terminated because of the temperature cap of 2000 K being exceeded, whereas the remainder proceeded for the full 10 applications of the $\times 5$ filter.

Figure 14 shows the conformational space sampled during the standard MD trajectory. Only the ϕ_3, ψ_2, ψ_3, and ψ_4 dihedral angles are sampled more than a small amount. In addition, no sampling of ϕ_2 is observed which is consistent with it being constrained by the proline ring.

Figure 15 plots the conformational space sampled by the RDFMD trajectory. In comparison with the MD trajectory, the sampling has clearly been increased in the ψ_1, ϕ_3, and ϕ_4 dihedrals. The $\psi-\phi$ sampling in the MD and RDMFD simulations is more complete than that observed by Wu and Wang in their MD and SGMD simulations; however, our MD simulation is twice as long. These plots are of limited use as they only show correlation between pairs of dihedrals; it is not possible to link a point on one of the quadrants with the corresponding point on the other three quadrants. They do not therefore give a complete picture of the secondary structure.

Figures 16 and 17 show hydrogen bond and secondary structure analyses of the MD and RDFMD trajectories, respectively. The analyses were performed using the DSSP algorithm[51] with the default hydrogen bond energy cutoff of -0.5 kcal mol^{-1}. In the analysis of the MD trajectory, a bend at 3 GLY and two short-lived turns were detected. By comparison, the RDFMD trajectory found a wider range of hydrogen bonds,

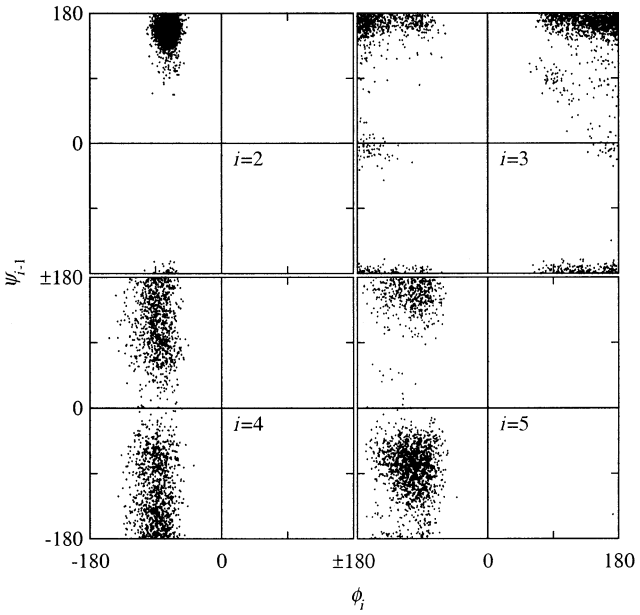

Figure 14. Backbone dihedral angle space sampled during the 4 ns MD simulation of YPGDV.

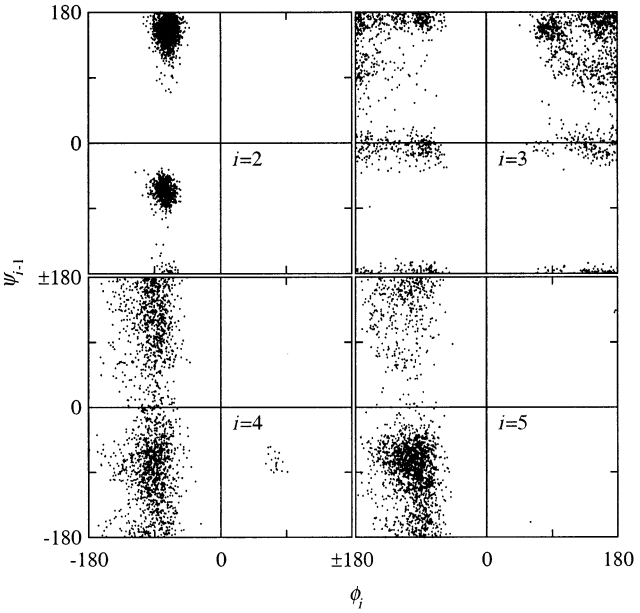

Figure 15. Backbone dihedral angle space sampled during the 2 ns RDFMD simulation of YPGDV.

more configurations contained hydrogen bonds, and more configurations contained turns and bends. Thus, the RDFMD trajectory is more consistent with the NMR results, in which approximately 50% of the conformations observed are expected to be β turns.

NOE intensities for the MD and RDFMD simulations were calculated and assigned according to the algorithm described by Wu and Wang[43] and are presented in Table 5. The MD and RDFMD simulations yielded very similar results, despite the difference in the conformations sampled and the hydrogen bonds and secondary structure observed. The results for both MD and RDFMD are more consistent with experiment than those reported for the SGMD simulation.

3.3.5. Summary. The system was set up to mimic as closely as possible the system used by Wu and Wang for their SGMD simulations. An initial simulation was performed to determine what design of filter was required for amplifying conformational

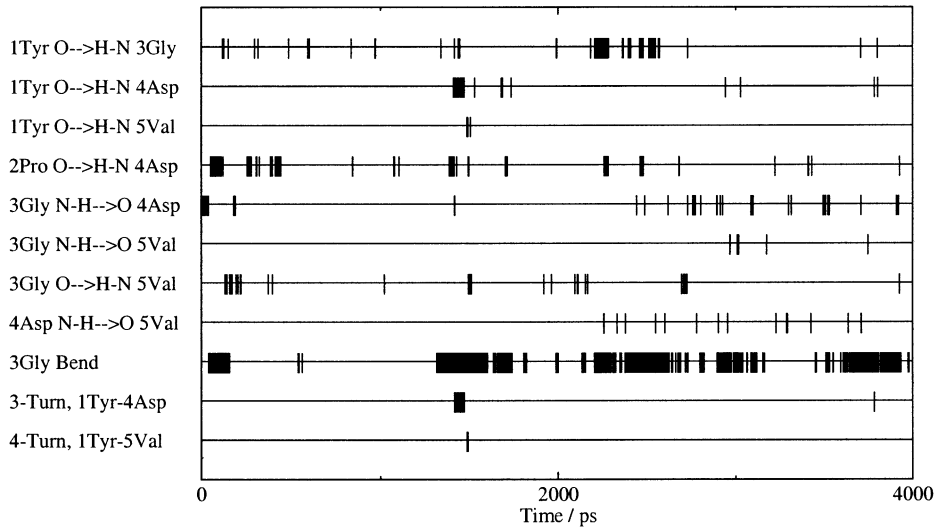

Figure 16. Hydrogen bonds and secondary structure elements present in the 4 ns MD simulation.

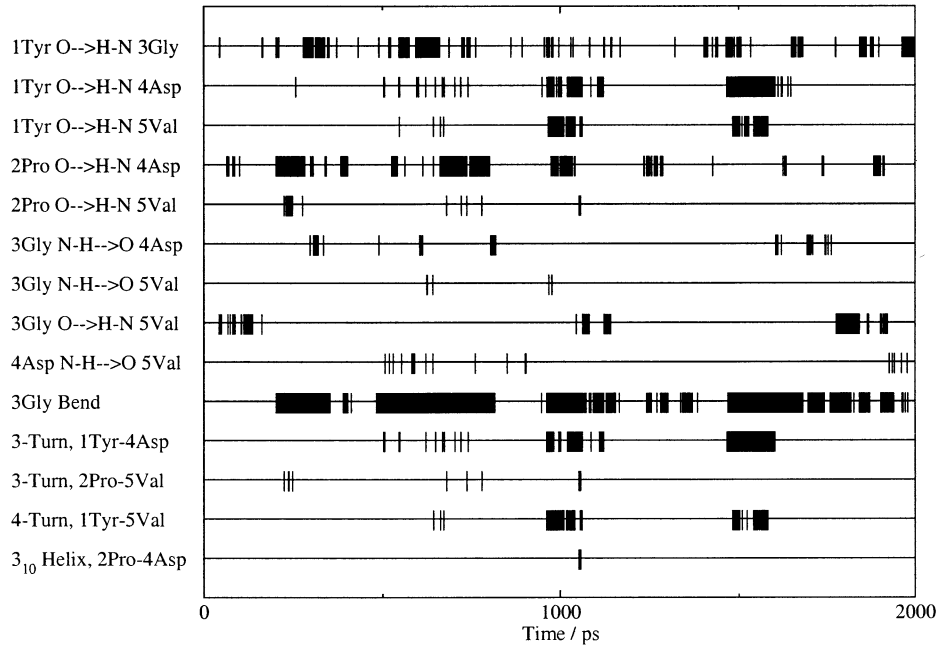

Figure 17. Hydrogen bonds and secondary structure elements present in the 2 ns RDFMD simulation.

TABLE 5: Experimental and Calculated NOE Intensities and Assignments for YPGDV

connectivity	experiment	MD	RDFMD	SGMD
$d_{\alpha N}(2, 3)$	s	3.390 (s)	3.398 (s)	8.540 (s)[b]
$d_{\alpha N}(3, 4)$	m	2.835 (s)	2.418 (s)	2.240 (s)
$d_{\alpha N}(3, 4)$[c]	m	2.853 (s)	2.804 (s)	
$d_{\alpha N}(4, 5)$[d]	s	1.438 (s)	1.356 (s)	3.380 (s)
$d_{\alpha N}(2, 4)$	w	0.053 (w)	0.064 (w)	0.240 (m)
$d_{NN}(3, 4)$	s[e]	1.015 (s)	1.130 (s)	0.880 (m)

[a] An NOE $\geq$ 1 is assigned "strong", 1 > NOE $\geq$ 0.18 is "medium" and 0.18 > NOE $\geq$ 0.05 is "weak". [b] This intensity was assigned "very strong" in the original SGMD paper. [c] The original spectrum has two medium intensity peaks for this resonance arising from the two C_α protons on 3GLY. The SGMD paper quotes just one computed value. [d] The $d_{\alpha N}(4, 5)$ peak is not listed in the original paper by Dyson et al. because it provides no insight into the structure of the turn. This NOE is strong in any unstructured peptide. [e] This peak is assigned as "strong" by Dyson et al. but as "medium" by Wu and Wang.

change, and a study of the energy dissipation half-life was made to determine the delay between filter applications. These studies resulted in a 0−25 cm^{-1} amplifying filter with a 20 step delay.

A simple protocol inducing conformational change was designed, employing an internal temperature cutoff to prevent conformational change in ω. A 2 ns RDFMD simulation using this protocol was performed and compared to the MD and SGMD trajectories (where possible). It was found that the configurations generated during the RDFMD experiment contained more secondary structure elements than for MD, that conformational change events often occurred soon after the filter application, and that the structures observed from the RDFMD trajectory were more consistent with experiment. The overhead associated with the RDFMD filter applications can be judged by looking at the number of simulation time steps needed for the filter applications, compared to the number of NPT time steps simulated between the filter applications. Where one hundred 20 ps NPT simulations were performed (1 000 000 time steps), 1 033 100 time steps were needed for the filter applications, an overhead of 103%. The CPU time required to apply the filters is negligible. Thus, for a fair comparison with the MD simulations, a 4 ns MD run was used, this being approximately equivalent to the total RDFMD simulation time.

4. Conclusion

The limitations of the DFMD method are the difficulty in targeting low-frequency oscillations in systems where energy dissipation is rapid (e.g., condensed phase systems) and the requirement to introduce all of the energy into the system in a single multiple-pulse filter application. The RDFMD method improves on the DFMD method by applying the filter to trajectories sampled both forward and backward in time. This enables the user to choose exactly where in the trajectory the filter is applied. By choosing to space filter applications closely in the trajectory, one filter application may build on the energy input and enhanced trajectory of a previous application in a way that is not possible with DFMD. The RDFMD method thus provides a mechanism for introducing frequency-targeted energy into the system in a gradual manner.

The RDFMD method has been applied to a single molecule of alanine dipeptide, solvated alanine dipeptide, and solvated YPGDV. The alanine dipeptide simulations (for which the adiabatic potential energy surface was calculated) showed a change in the characteristic frequency of the target mode as energy was gradually introduced into the system. The change in the frequency was compensated for by using a succession of different filters. It was also determined that the ϕ and ψ angles in alanine dipeptide oscillated with different frequencies, and the frequency-specific nature of the RDFMD method was demonstrated by causing transitions driven by either ϕ or ψ. Reasonable conformational transitions were successfully induced in this system.

Successful conformational change events via a variety of different transition paths were induced in alanine dipeptide solvated in chloroform from 9 out of 10 different start points. The energy introduced into the system for each conformational change was reproduced using a heating pulse. No conformational transitions were produced by adding the same amount of energy into the system in this non frequency-specific manner.

Finally, the RDFMD method was applied to the pentapeptide solvated in water. In this case, the underlying energy hypersurface was not known, and hence, a protocol for performing an NPT simulation with regular RDFMD filter applications was devised. The resulting trajectory was compared with a normal MD trajectory and with limited data on the SGMD trajectory for the same system. A greater variety of configurations were generated during the RDFMD experiment and more defined secondary structure was seen than in the MD trajectory.

Acknowledgment. S.C.P. and M.T.S. would like to thank GlaxoSmithKline for their generous support. J.W.E. is a Royal Society University Research Fellow. This work is supported by the EPSRC and the BBSRC.

References and Notes

(1) Gerstein, M.; Krebs, W. *Nucleic Acids Res.* **1998**, *26*, 4280−4290.
(2) Czerminski, R.; Elber, R. *J. Chem. Phys.* **1990**, *92*, 5580−5601.
(3) Smart, O. S. *Chem. Phys. Lett.* **1994**, *222*, 503−512.
(4) Fischer, S.; Karplus, M. *Chem. Phys. Lett.* **1992**, *194*, 252−261.
(5) Schlitter, J.; Engels, M.; Kruger, P. *J. Mol. Graphics* **1994**, *12*, 84−89.
(6) Amadei, A.; Linssen, A. B. M.; de Groot, B. L.; van Aalten, D. M. F.; Berendsen, H. J. C. *J. Biomol. Struct. Dyn.* **1996**, *13*, 615−625.
(7) Abseher, R.; Nilges, M. *Proteins* **2000**, *39*, 82−88.
(8) Grubmuller, H. *Phys. Rev. E* **1995**, *52*, 2893−2906.
(9) Mitsutake, A.; Sugita, Y.; Okamoto, Y. *Biopolymers* **2001**, *60*, 96−123.
(10) Phillips, S. C.; Essex, J. W.; Edge, C. M. *J. Chem. Phys.* **2000**, *112*, 2586−2597.
(11) Dauber-Osguthorpe, P.; Maunder, C. M.; Osguthorpe, D. J. *J. Comput.-Aided Mol. Design* **1996**, *10*, 177−185.
(12) Williams, C. S. *Designing Digital Filters*; Prentice Hall: Englewood Cliffs, NJ, 1986.
(13) MATLAB 5.3.0; The MathWorks Inc.: Natick, MA, 1999.
(14) Allen, M. P.; Tildesley, D. J. *Computer Simulation of Liquids*; Oxford University Press: Oxford, U.K., 1987.
(15) Huang, N. E.; Shen, Z.; Long, S. R.; Wu, M. L. C.; Shih, H. H.; Zheng, Q. N.; Yen, N. C.; Tung, C. C.; Liu, H. H. *Proc. R. Soc. London Ser. A-Math. Phys. Eng. Sci.* **1998**, *454*, 903−995.
(16) Phillips, S. C.; Gledhill, R. J.; Essex, J. W.; Edge, C. M. *J. Phys. Chem. A* Submitted.
(17) Sessions, R. B.; Dauber-Osguthorpe, P.; Osguthorpe, D. J. *J. Mol. Biol.* **1989**, *210*, 617−633.
(18) Dauber-Osguthorpe, P.; Osguthorpe, D. J. *J. Am. Chem. Soc.* **1990**, *112*, 7921−7935.
(19) Sessions, R. B.; Osguthorpe, D. J.; Dauber-Osguthorpe, P. *J. Phys. Chem.* **1995**, *99*, 9034−9044.
(20) Melchionna, S.; Cozzini, S. *DLPROTEIN 1.2.*; Unità di Roma "La Sapienza": Rome, Italy, 1997.
(21) Olender, R.; Elber, R. *J. Chem. Phys.* **1996**, *105*, 9299−9315.
(22) Wu, X. W.; Wang, S. M. *J. Phys. Chem. B* **1998**, *102*, 7238−7250.
(23) Kleinjung, J.; Bayley, P.; Fraternali, F. *Febs Lett.* **2000**, *470*, 257−262.
(24) Pettitt, B. M.; Karplus, M. *Chem. Phys. Lett.* **1985**, *121*, 194−201.
(25) Marrone, T. J.; Gilson, M. K.; McCammon, J. A. *J. Phys. Chem.* **1996**, *100*, 1439−1441.
(26) Bartels, C.; Karplus, M. *J. Comput. Chem.* **1997**, *18*, 1450−1462.
(27) Scarsi, M.; Apostolakis, J.; Caflisch, A. *J. Phys. Chem. B* **1998**, *102*, 3637−3641.
(28) Smith, P. E. *J. Chem. Phys.* **1999**, *111*, 5568−5579.
(29) Anderson, A. G.; Hermans, J. *Proteins* **1988**, *3*, 262−265.
(30) Lazaridis, T.; Tobias, D. J.; Brooks, C. L.; Paulaitis, M. E. *J. Chem. Phys.* **1991**, *95*, 7612−7625.
(31) Apostolakis, J.; Ferrara, P.; Caflisch, A. *J. Chem. Phys.* **1999**, *110*, 2099−2108.
(32) Jorgensen, W. L. *BOSS 4.1.*; Yale University, New Haven, CT, 1999.
(33) Jorgensen, W. L.; Tirado-Rives, J. *J. Am. Chem. Soc.* **1988**, *110*, 1657−1666.
(34) Ryckaert, J. P.; Ciccoti, G.; Berendsen, H. J. C. *J. Comput. Phys.* **1977**, *23*, 327−341.
(35) Jorgensen, W. L.; Briggs, J. M.; Contreras, M. L. *J. Phys. Chem.* **1990**, *94*, 1683−1686.
(36) Essex, J. W. *Free Energy Calculations in Molecular Biology*. Ph.D. Thesis, Oriel College, Oxford, 1992.
(37) Melchionna, S.; Ciccotti, G.; Holian, B. L. *Mol. Phys.* **1993**, *78*, 533−544.
(38) Dyson, H. J.; Rance, M.; Houghten, R. A.; Lerner, R. A.; Wright, P. E. *J. Mol. Biol.* **1988**, *201*, 161−200.
(39) Tobias, D. J.; Mertz, J. E.; Brooks, C. L. *Biochemistry* **1991**, *30*, 6054−6058.
(40) Brooks, B. R.; Bruccoleri, R. E.; Olafson, B. D.; States, D. J.; Swaminathan, S.; Karplus, M. *J. Comput. Chem.* **1983**, *4*, 187−217.
(41) Jorgensen, W. L.; Chandrasekhar, J.; Madura, J. D.; Impey, R. W.; Klein, M. L. *J. Chem. Phys.* **1983**, *79*, 926−935.
(42) Karpen, M. E.; Tobias, D. J.; Brooks, C. L. *Biochemistry* **1993**, *32*, 412−420.
(43) Wu, X. W.; Wang, S. M. *J. Phys. Chem. B* **2000**, *104*, 8023−8034.
(44) Mackerell, A. D.; Bashford, D.; Bellott, M.; Dunbrack, R. L.; Evanseck, J. D.; Field, M. J.; Fischer, S.; Gao, J.; Guo, H.; Ha, S.; Joseph-Mccarthy, D.; Kuchnir, L.; Kuczera, K.; Lau, F. T. K.; Mattos, C.; Michnick, S.; Ngo, T.; Nguyen, D. T.; Prodhom, B.; Reiher, W. E.; Roux, B.; Schlenkrich, M.; Smith, J. C.; Stote, R.; Straub, J.; Watanabe, M.; Wiorkiewicz-Kuczera, J.; Yin, D.; Karplus, M. *J. Phys. Chem. B* **1998**, *102*, 3586−3616.
(45) Jorgensen, W. L. *MCPRO 1.4.*; Yale University, New Haven, CT, 1996.
(46) Jorgensen, W. L.; Maxwell, D. S.; Tirado-Rives, J. *J. Am. Chem. Soc.* **1996**, *118*, 11225−11236.
(47) Kale, L.; Skeel, R.; Bhandarkar, M.; Brunner, R.; Gursoy, A.; Krawetz, N.; Phillips, J.; Shinozaki, A.; Varadarajan, K.; Schulten, K. *J. Comput. Phys.* **1999**, *151*, 283−312.
(48) Darden, T.; York, D.; Pedersen, L. *J. Chem. Phys.* **1993**, *98*, 10089−10092.
(49) Paterlini, M. G.; Ferguson, D. M. *Chem. Phys.* **1998**, *236*, 243−252.
(50) Feller, S. E.; Zhang, Y. H.; Pastor, R. W.; Brooks, B. R. *J. Chem. Phys.* **1995**, *103*, 4613−4621.
(51) Kabsch, W.; Sander, C. *Biopolymers* **1983**, *22*, 2577−2637.